Membrane Mediated Interactions between Peptides. 1. Finite Difference Technique and Two-Body Interaction

M.B. Partenskii, G.V. Miloshevsky, P.C. Jordan

Department of Chemistry, Brandeis University, Waltham, MA 02454, USA

Abstract

Membrane mediated interactions between inclusions arise from perturbation of the membrane at the lipid-peptide interface. A finite difference algorithm was developed to numerically calculate the distortion of the membrane due to the insertion of proteins. We outline a scheme that permits a small grid spacing, δl ~ 0.4 Å, while maintaining computational efficiency and test it by comparing results with those known for a single inclusion, as functions of the contact slope s, the gradient of the deformation profile at the interface. For δl between 0.5 and 2.0 Å, the deformation profiles, $u(r)$, reproduce previous results [1,2,4]. However, the deformation free energy, $F(s)$, is sensitive to δl. For δl = 0.5 Å, reasonable (to within 5%) agreement was found for the physically most important s-domain, $-0.2 < s < 0.0$. We study membrane-mediated interactions between two cylindrical inclusions as a function of both s and the separation distance d. When minimized as a function of s (in some cases permitting azimuthal variation) the free energy, $F_{min}(d)$, is repulsive. However, with s fixed, the profiles $F(d)$ exhibit van der Waals-like transitions from attractive (for $s > s_{cr1}$) to repulsive behavior (for $s < s_{cr2}$); in the intermediate region, the profiles are sigmoidal in d. The optimized interaction between two proteins is repulsive at all separations if the slope is assumed to be azimuthally symmetrical. However, allowing slope to adjust its azimuthal dependence creates an attractive region at distances d <15 Å, separated by the barrier from the repulsive region.

Elastic Energy, Euler-Lagrange Equation and Boundary Conditions

In simple models for peptide insertion into a membrane the elastic free energy arises from the vertical displacement, u_0, of lipid molecules in immediate contact with a (cylindrical) inclusion of radius r_0 [1]. A membrane's elastic free energy containing bending and stretching contributions is expressed as [2]

$$E = 2\pi \int d^2\mathrm{r}[b(\mathrm{r})(\Delta u)^2 + a(\mathrm{r})u(\mathrm{r})^2] \qquad (1)$$

with

$$a(\mathrm{r}) = 2B(\mathrm{r})/h_0, \qquad b(\mathrm{r}) = h_0 K(\mathrm{r})/2$$

where $\mathrm{r} = (x,y)$ is the radius-vector in the plane of the membrane; $B(\mathrm{r})$ and $K(\mathrm{r})$ are stretching and bending constants which in general depend on r, h_0 is the unperturbed hydrophobic membrane thickness. The variational solution to Eq. 1 yields an Euler-Lagrange equation for $u(x,y)$

$$\Delta(b(x,y)\Delta u(x,y)) + a(x,y)u(x,y) = 0 \qquad (2)$$

Its solution is a boundary value problem. For finite-size inclusion clusters far from the membrane boundaries, both $u(\mathrm{r})$ and $\nabla u(\mathrm{r}) \rightarrow 0$ at the edge of the computational domain:

$$u|_{ext} = \nabla u|_{ext} = 0 \qquad (3)$$

At the internal boundaries, L, the membrane is in contact with an inclusion and $u(\mathrm{r})$ is fixed at u_o. Furthermore, the contact slope $s = \nabla u(\mathrm{r}_L)$ is fixed. It need not be constant; in general its functional variation along the interface is prescribed. Thus

$$u(\mathrm{r}_L) = u_0, \qquad \nabla u(\mathrm{r}_L) = s(\mathrm{r}_L) \tag{4}$$

where r_L is an arbitrary point on the internal boundary. In most cases, $s(\mathrm{r}_L)$ is assumed isotropic, and either fixed ("constrained" boundary condition [1,3])

$$s(\mathrm{r}_L) = s = const \tag{5}$$

or chosen from the minimum of $E(s)$ ("relaxed" condition [3,4])

$$s = s_{min}. \tag{6}$$

Eqs. 2-4 are then solved numerically using a finite difference representation on a two-dimensional mesh.

Testing the algorithm – a single inclusion

We tested the numerical technique for a single cylindrically symmetric inclusion for both uniform and non-uniform cases. Non-uniform elastic constants are estimated as

$$B(r) = B_0T(r),\ K(r) = K_0T(r) \qquad \text{with} \qquad T(r) \equiv 1 + (\theta\text{-}1)\exp[-2(r\text{-}r_0)/h_0].$$

B_0 and K_0 are the elastic constants of a neat membrane; θ accounts for elastic constant perturbation by the inclusion. θ is set to 1 (the uniform case) or 4 (which accounts for experimental lifetimes of gramicidin A channels [2]). Calculations were carried out at 300 K for mesh spacings, δl, of 0.5, 1 & 2 Å for GA channel in various membranes. We compare results for ***DMPC*** membranes (u_0 = 1.65 Å) with those computed analytically or numerically. The differences are small (< 2% error) for all δl and both θ. The total deformation free energy is more sensitive to δl.

Fig. 1 compares free energy profiles as functions of contact slope. The agreement between mesh and reference results is especially good in the slope range (-0.2 to 0.0). Interestingly, changing δl has only minor effect in the slope range (-0.1, 0.0). Errors increase for larger negative slopes.

Fig. 2 depicts energy dependence on inclusion radius, r_0. For s = 0 mesh and exact solutions [1,2] agree perfectly. If energy is optimized over s, agreement is good for sufficiently large radii, $r_0 > 5$ Å, but fails as $r_0 \to 0$, since analytically, $s \to \infty$ near inclusions. However, such small r_0 have no practical implications.

Two inclusions

We have solved the uniform (θ = 1) elastic problem for two inclusions at various separations d (the minimal intersurface distance), setting u_0 = 1.65 Å and varying s. The slope s is assumed cylindrically symmetrical. The deformation profiles along the line connecting the inclusion centers are presented in **Fig. 3** for $s = s_{min}$.

For relaxed boundary conditions $s = s_{min}$ with cylindrically symmetrical slope the elastic interaction between two inclusions is repulsive (**Fig. 4**). The inclusion radii are 10.0 Å. The free energy profiles are shown as functions of the separation distance between two inclusions.

Fig. 5 presents deformational free energy profiles $F(d)$ for various cylindrically symmetrical contact slopes s ($-0.2 \le s \le 0$). They exhibit van der Waals type behavior. Interaction is repulsive at larger slopes, $s \ge s_{cr1} \approx -0.03$. In the intermediate region, $-0.08 \le s \le s_{cr1} \approx -0.03$, a minimum exists at finite inter-inclusion distances, separated by a barrier from the large d region. Interaction becomes attractive at small s, $s \le s_{cr2} \approx -0.08$.

These results may be physically significant if the slope s is really controllable by an inclusion. This implies the peptides' clustering behavior could change with changes in the membrane's lipid composition (phase transition).

We tested the validity of assuming that the contact slope is cylindrically symmetric and approximated the slope by a trial function

$$s(\phi) = s + s_1 \cos(\phi); \qquad (7)$$

s and s_1 are parameters and ϕ is the "azimuthal" angle. Thus $s(\phi)$ is larger on the inter-inclusion side and symmetrically smaller on the outer side. We also considered a family of functions allowing asymmetric variation of s

$$s_n(\phi) = s + s_1\{1/[1 + \phi^n] - R(n)\}/(1-R(n)) \qquad (8)$$

with

$$R(n)^{-1} = \pi^{-1} \int_0^{\pi} d\phi\{1/[1 + \phi^n]\}.$$

The deformational free energy per inclusion as a function of s_1 is shown in **Fig. 6** (for $s(\phi)$ given by Eq. 7) for the average slope minimized for each distance ($s = s_{min}$) and in **Fig. 7** for $s = 0$. Increasing s_1 initially reduces the free energy. The optimal value of s_1 depends on d. Eq. 8 yields similar results although for $n = 2$ and $n = 3$ the reduction of free energy is more effective than with functional form of Eq. 7 (**Figs. 8 & 9**).

At small separations (d <20 Å) anisotropy significantly reduces the free energy, and makes the interaction between the inclusions attractive. However, at large distances (d > 15 Å) the effect is insignificant.

Conclusions

1) We developed a computationally effective algorithm for the numerical solution of the variational elastic problem for any number of inclusions.
2) We showed that for physically meaningful inclusion radii and contact slopes, this algorithm provides highly accurate deformation fields and energies.
3) The two-body interaction between the inclusions has been studied as a function of their separation, d, and for different contact slopes, s. The profiles $F(d)$ exhibit van der Waals type transitions from attractive (for $s > s_{cr1}$) to repulsive (for $s > s_{cr2}$) behavior for cylindrically symmetrical slope; in the intermediate region, profiles are sigmoidal in d. If the interfacial slope is controllable and if it varies with lipid composition, and identifying d with the average (concentration dependent) distance between the inclusions, critical behavior in the lipid composition-inclusions concentration phase plane may arise, which calls for further investigation.
4) The slope anisotropy along the contour of the membrane-inclusion interface can significantly influence two-body interactions, even leading to the appearance of an attractive region at $d \leq 20$ Å. The reduction of energy at short distances can reach ~50%. All known elastic calculations with the isotropic s lead to strictly repulsive two-body interaction. Molecular model calculations [5] of the entropic force between two inclusions, however, predicted an attractive branch at short separations. The effect of anisotropy is negligible for $d > 20$ Å.

References

1. H. W. Huang, Biophys. J. **50**:1061-1070, 1986.
2. P. C. Jordan, G. V. Miloshevsky & M. B. Partenskii, In " Interfacial Catalysis," G. Volkov ed., Marcel Dekker, 2002 (in press)
3. C. Nielsen, M. Goulian & O. S. Andersen, Biophys. J. **74**:1966-1983, 1998.
4. P. Helfrich & E. Jakobsson, Biophys. J. **57**:1075-1084, 1990.
5. P. Lague, M. J. Zuckermann & B. Roux, Biophys. J. **79**:2867-2879, 2000

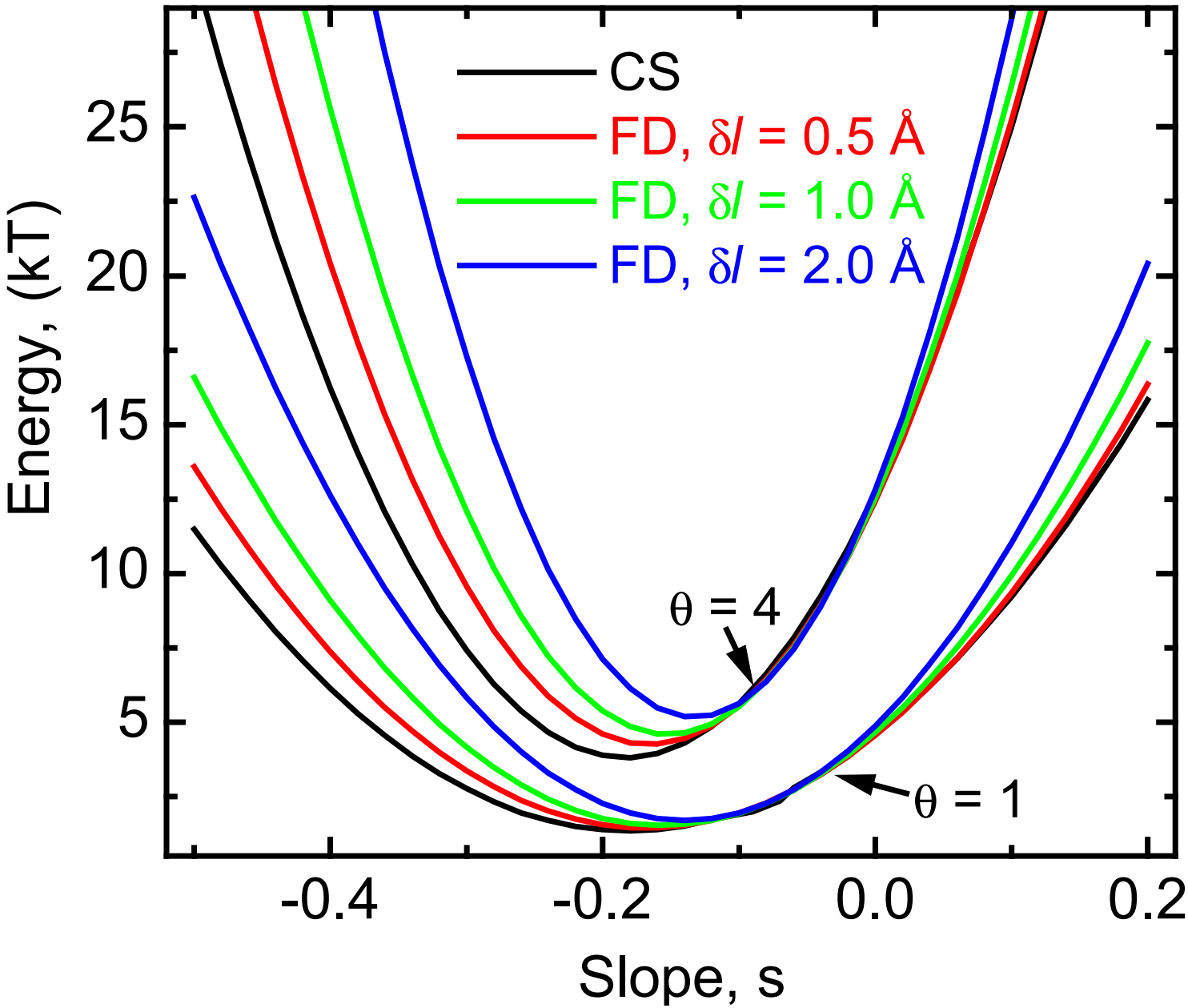

Fig. 1 Deformation free energies versus slope in the uniform (θ=1) and non-uniform (θ=4) cases. Exact (CS) results are compared with finite difference (FD) results obtained with a two-dimensional grid for different mesh spacings δl.

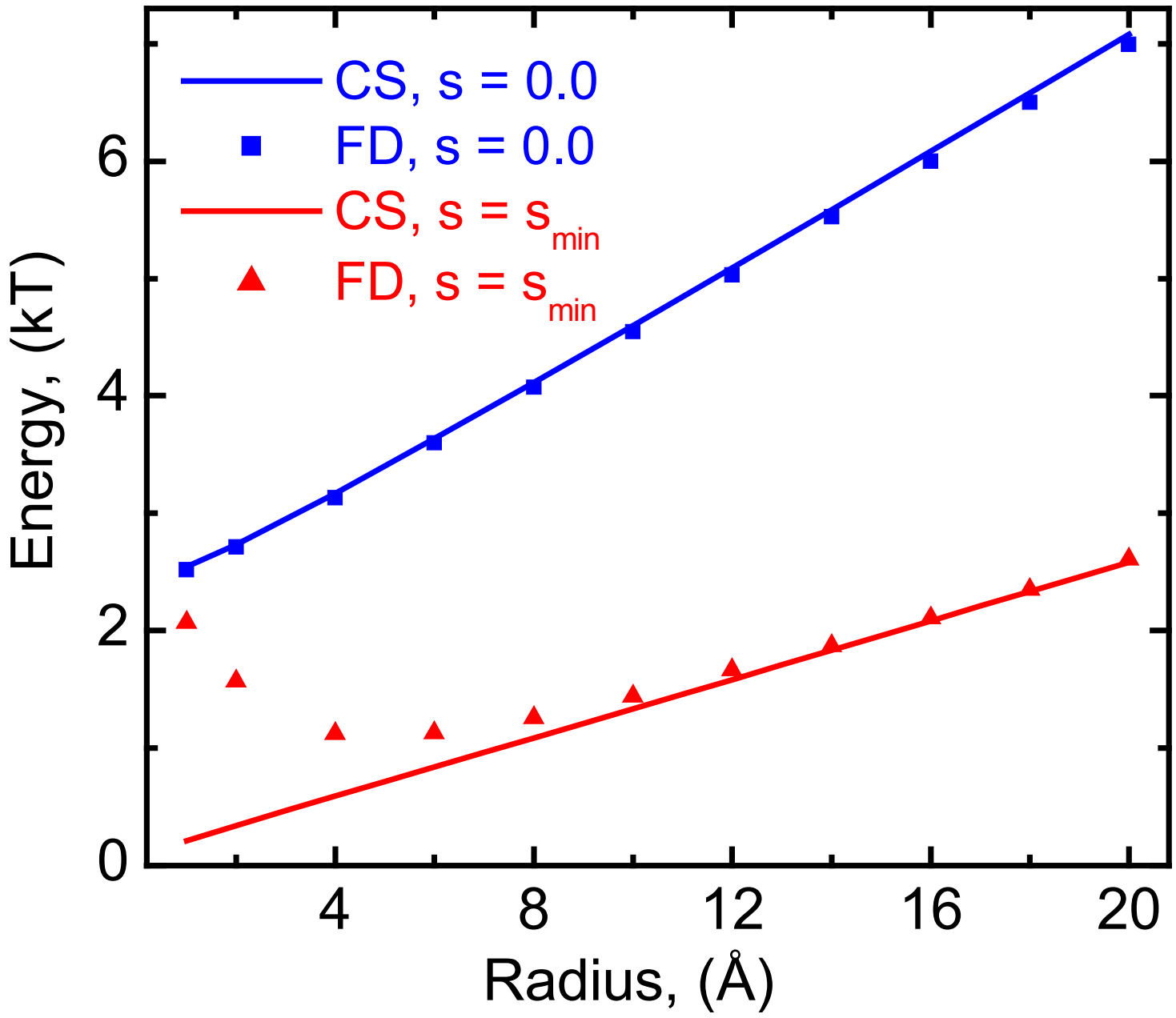

Fig. 2 Deformation free energy as a function of r_0 for $\theta = 1$. Comparisons are for $s = 0.0$ and $s = s_{min}$ (Eqs. 5 & 6). FD computations are for $\delta l = 0.5$ Å.

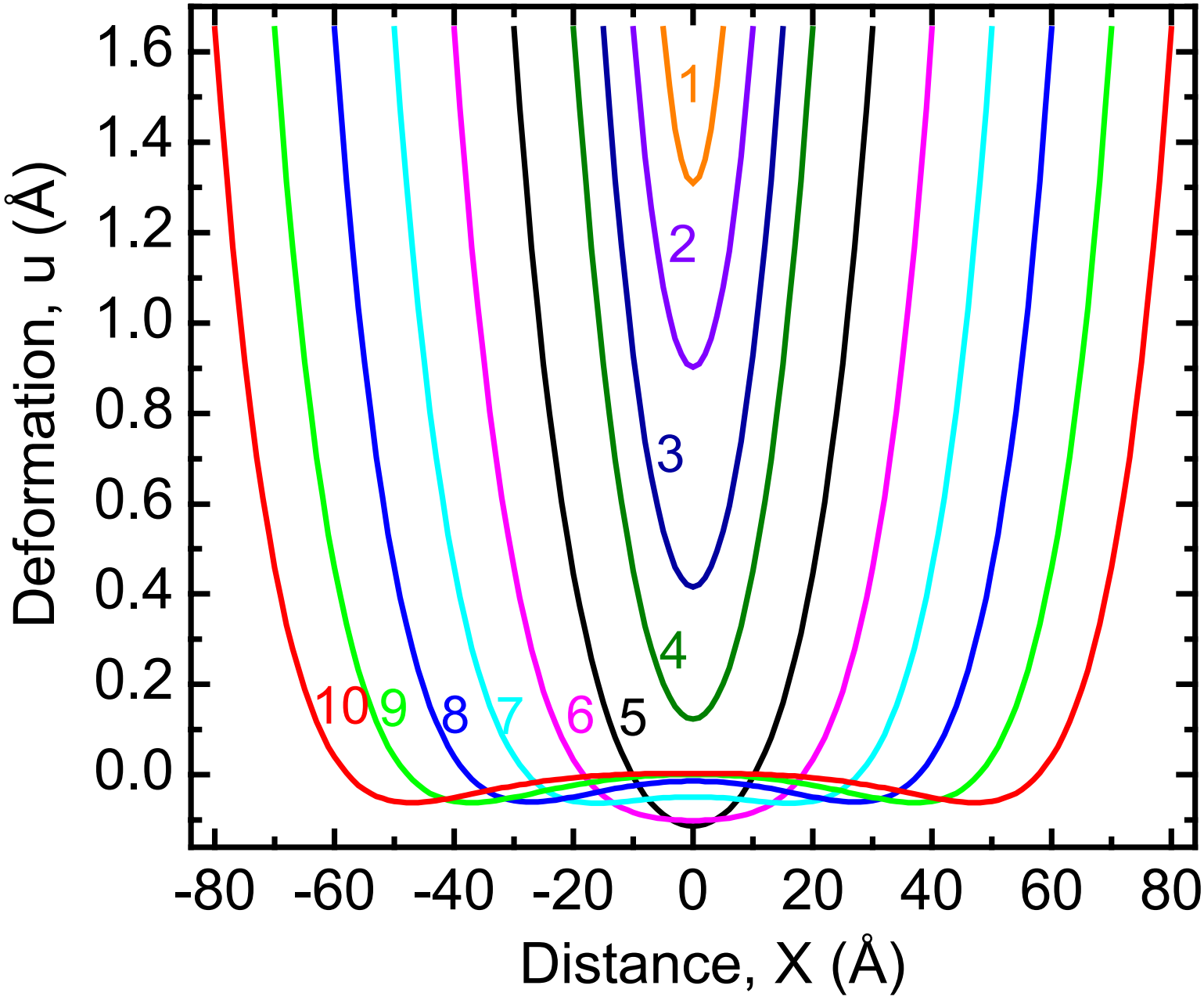

Fig. 3 Deformation profiles between two inclusions along the axis X, through the centers of the inclusions, for different separation distances d: (1) 10; (2) 20; (3) 30; (4) 40; (5) 60; (6) 80; (7) 100; (8) 120; (9) 140; (10) 160 Å.

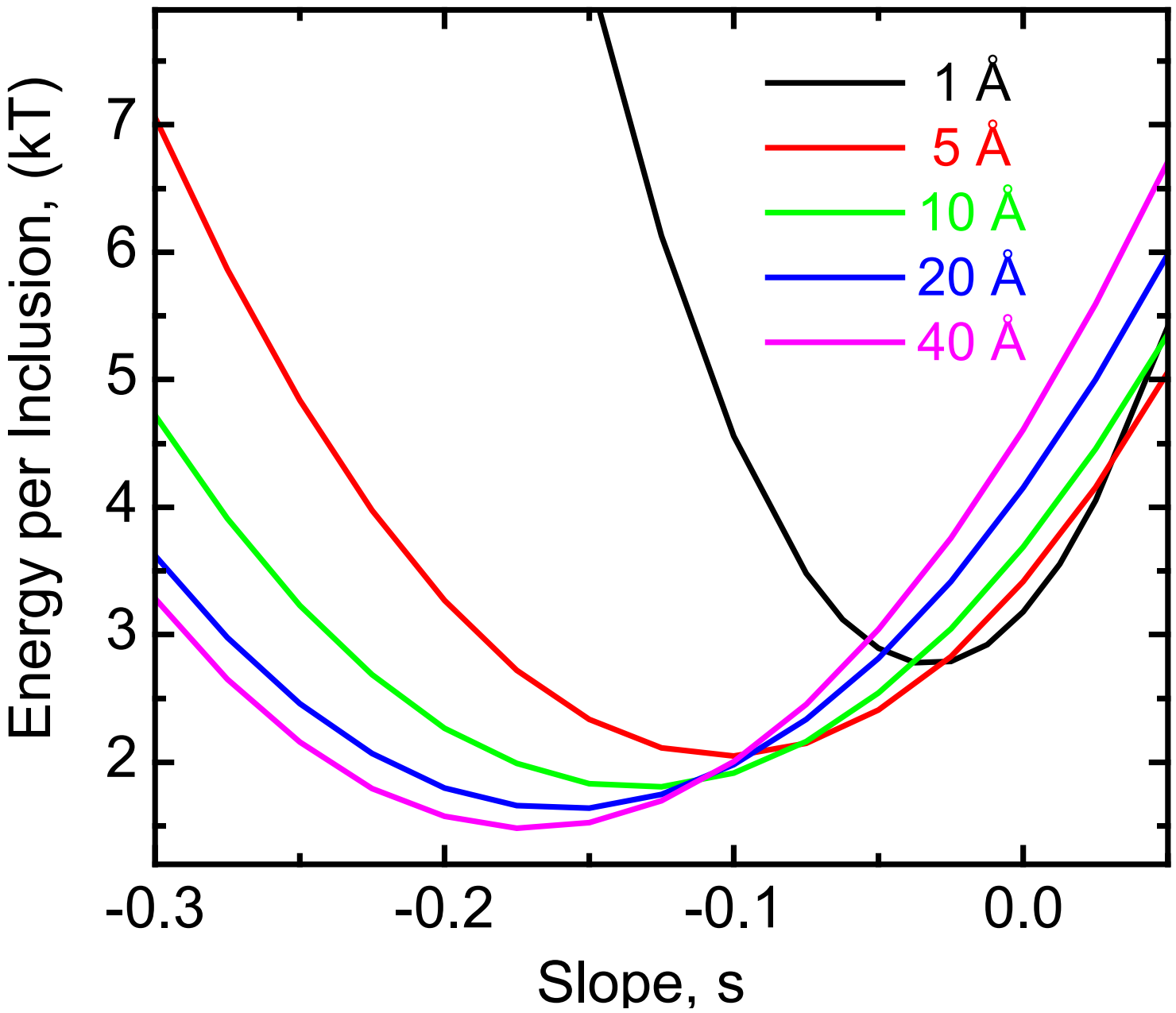

Fig. 4 Deformation free energy per inclusion for interaction of two peptides as a function of the contact slope s, for different separation distances d.

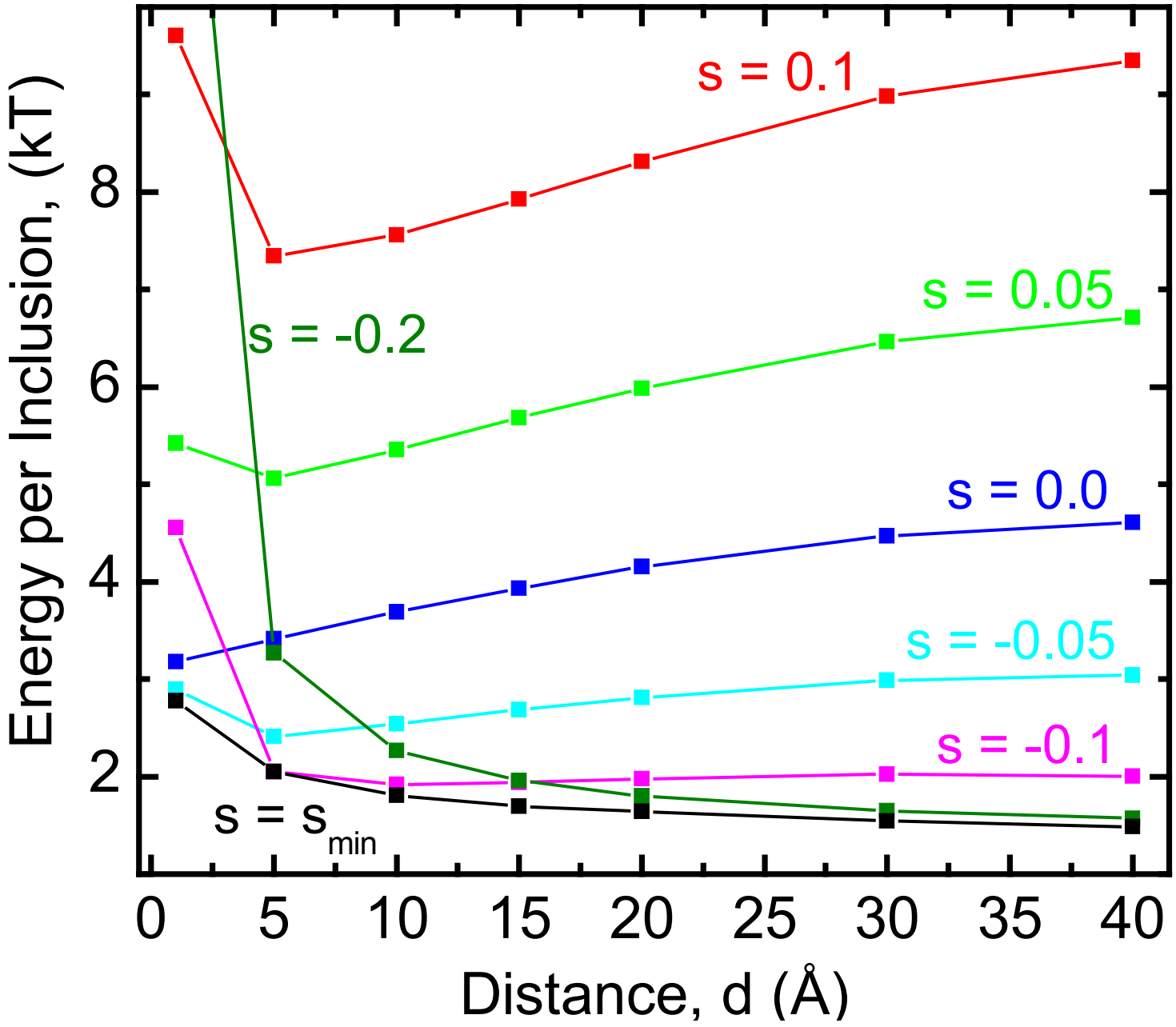

Fig. 5 Deformation energy profiles F(d), for different values of the contact slope s (assumed azimuthally symmetrical).

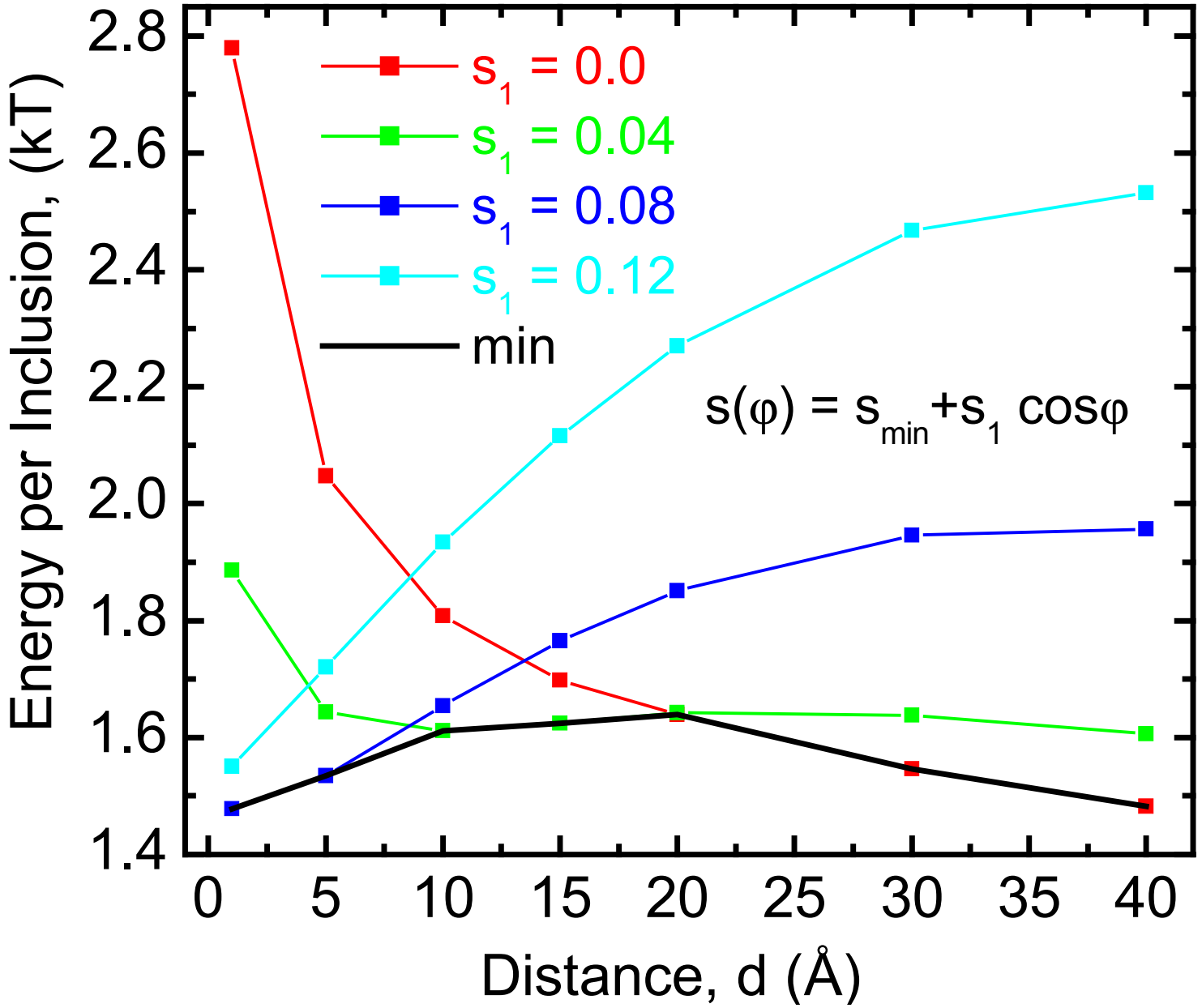

Fig. 6 Deformation energy profiles F(d), for asymmetric boundary slopes (Eq. 7), with mean slope fixed at $s=s_{min}$, for different values of s_1. Also shown (min) is the deformation energy minimized with respect to s_1.

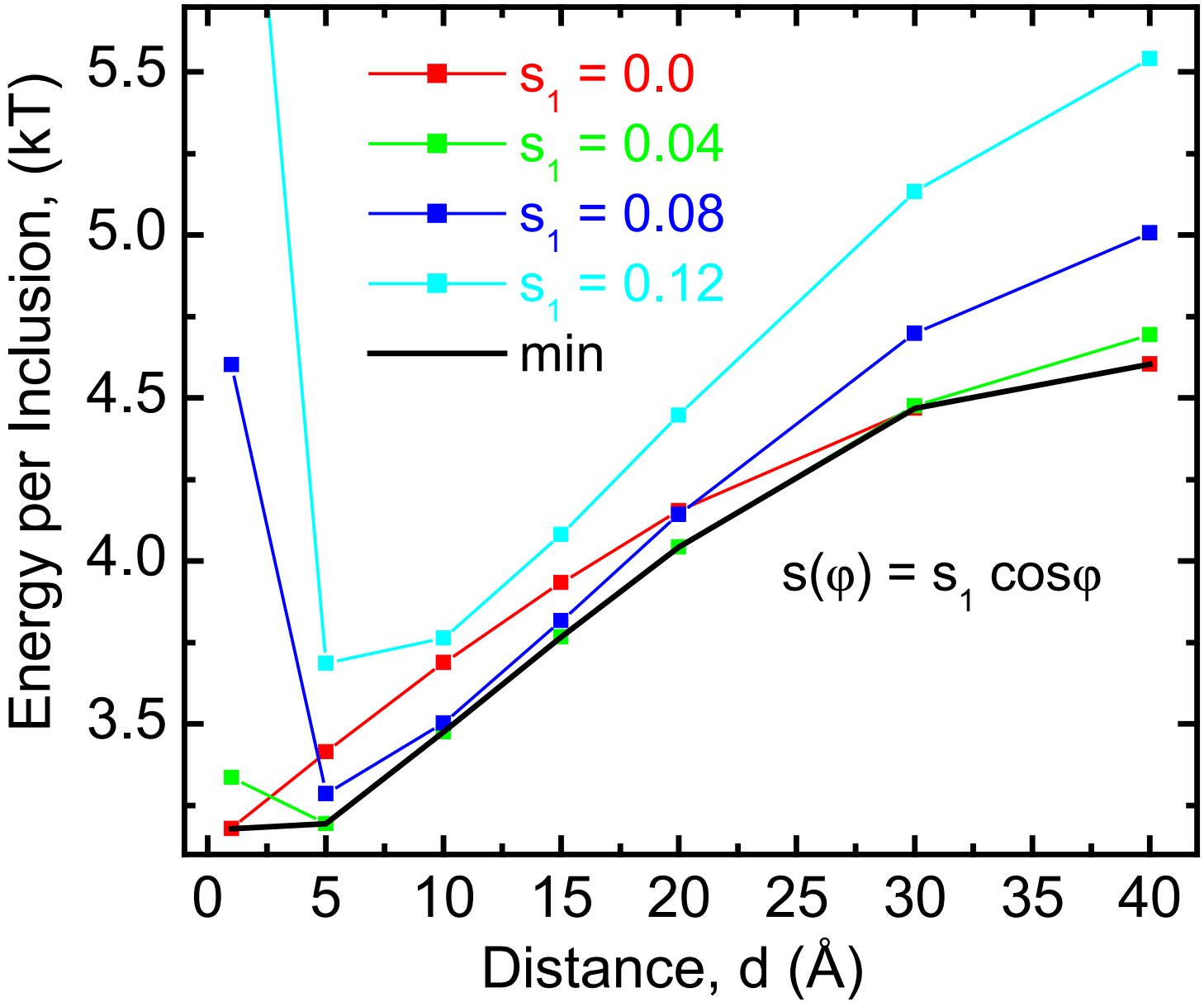

Fig. 7 Deformation energy profiles F(d), for asymmetric boundary slopes (Eq. 7) with mean slope fixed at s=0, for different values of s_1. Also shown (min) is the deformation energy minimized with respect to s_1.

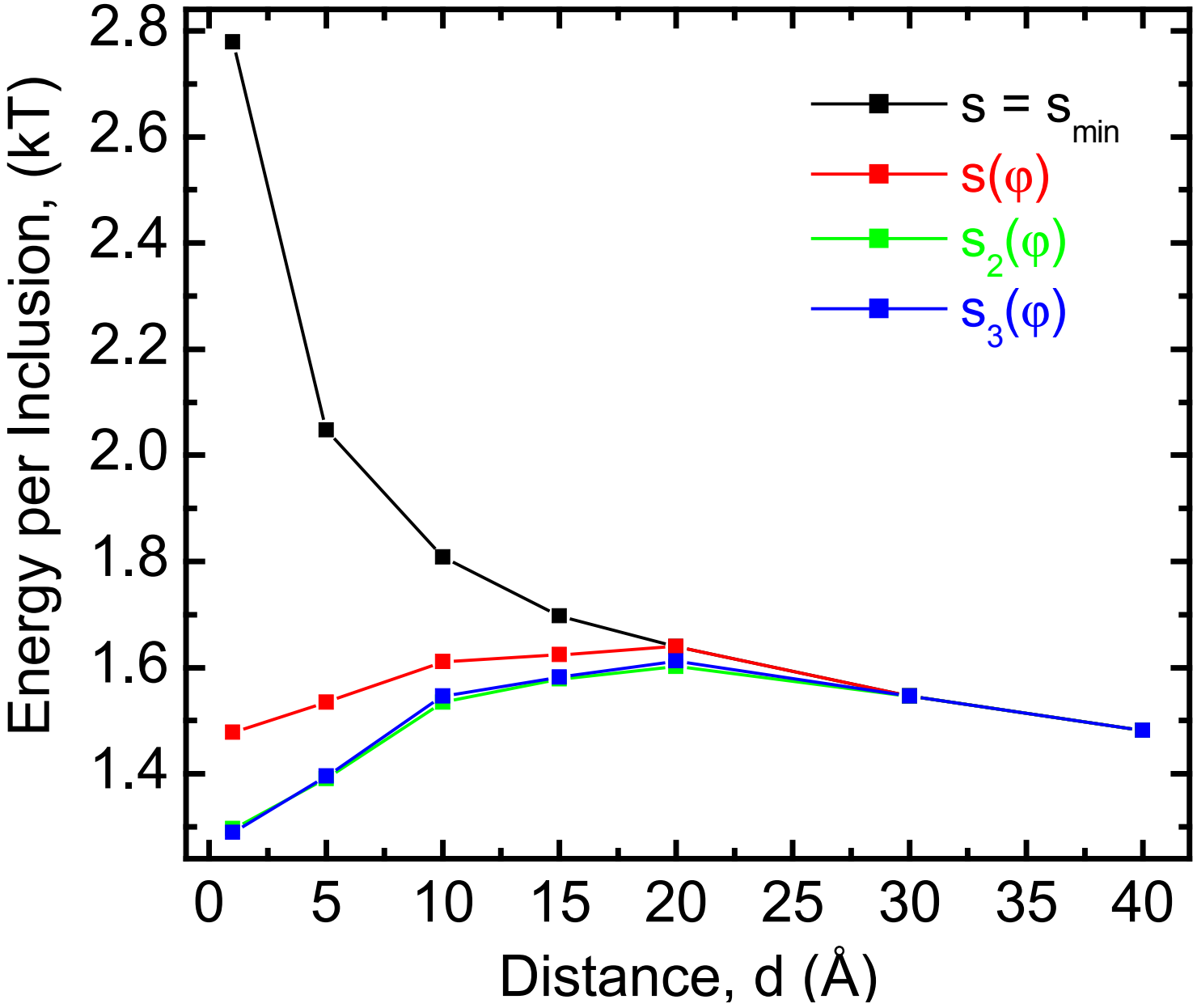

Fig. 8 The energy $F_{min}(d)$, minimized with respect to two parameters, s and s_1, for different functional forms of the asymmetric boundary slope, Eqs. 7 & 8. Also shown is the energy profile for the minimized isotropic slope.

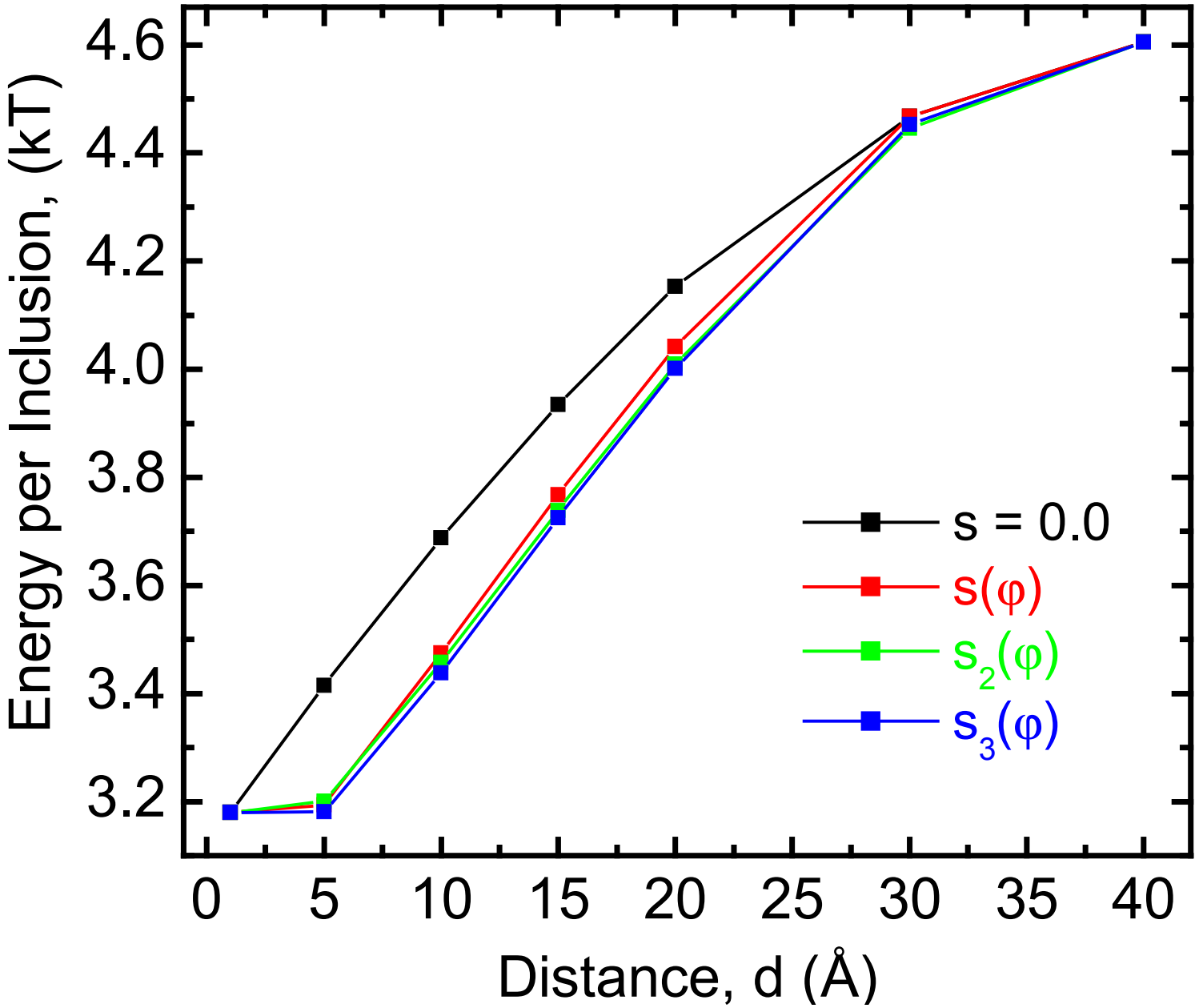

Fig. 9 Deformation energy profiles F(d), for different functional forms of the asymmetric boundary slope, Eqs. 7 & 8, minimized with respect to s_1, with mean slope s = 0.0 .